Determination of the Midpoint Potential of the FAD and FMN Flavin Cofactors and of the 3Fe−4S Cluster of Glutamate Synthase†

Sergio Ravasio,‡ Bruno Curti,‡ and Maria A. Vanoni*,‡,§

Dipartimento di Fisiologia e Biochimica Generali, Universitá degli Studi di Milano, Via Celoria 26, 20133 Milano, and Dipartimento di Scienze Chimiche Fisiche e Matematiche, Universitá degli Studi dell' Insubria, Via Valleggio II, 22100 Como, Italy

Received January 12, 2001; Revised Manuscript Received February 23, 2001

ABSTRACT: Glutamate synthase is a complex iron−sulfur flavoprotein that catalyzes the reductive transfer of the L-glutamine amide group to C(2) of 2-oxoglutarate, forming two molecules of L-glutamate. The bacterial enzyme is an $\alpha\beta$ protomer, which contains one FAD (on the β subunit, ∼50 kDa), one FMN (on the α subunit, ∼150 kDa), and three different Fe−S clusters (one 3Fe−4S center on the α subunit and two 4Fe−4S clusters at an unknown location). To address the problem of the intramolecular electron pathway, we have measured the midpoint potential values of the flavin cofactors and of the 3Fe−4S cluster of glutamate synthase in the isolated α and β subunits and in the $\alpha\beta$ holoenzyme. No detectable amounts of flavin semiquinones were observed during reductive titrations of the enzyme, indicating that the midpoint potential value of each $flavin_{ox}/flavin_{sq}$ couple is, in all cases, significantly more negative than that of the corresponding $flavin_{sq}/flavin_{hq}$ couple. Association of the two subunits to form the $\alpha\beta$ protomer does not alter significantly the midpoint potential value of the FMN cofactor and of the 3Fe−4S cluster (approximately −240 and −270 mV, respectively), but it makes that of FAD some 40 mV less negative (approximately −340 mV for the β subunit and −300 mV for FAD bound to the holoenzyme). Binding of the nonreducible $NADP^+$ analogue, 3-aminopyridine adenine dinucleotide phosphate, made the measured midpoint potential value of the FAD cofactor approximately 30−40 mV less negative in the isolated β subunit, but had no effect on the redox properties of the $\alpha\beta$ holoenzyme. This result correlates with the formation of a stable charge-transfer complex between the reduced flavin and the oxidized pyridine nucleotide in the isolated β subunit, but not in the $\alpha\beta$ holoenzyme. Binding of L-methionine sulfone, a glutamine analogue, had no significant effect on the redox properties of the enzyme cofactors. On the contrary, 2-oxoglutarate made the measured midpoint potential value of the 3Fe−4S cluster approximately 20 mV more negative in the isolated α subunit, but up to 100 mV less negative in the $\alpha\beta$ holoenzyme as compared to the values of the corresponding free enzyme forms. These findings are consistent with electron transfer from the entry site (FAD) to the exit site (FMN) through the 3Fe−4S center of the enzyme and the involvement of at least one of the two low-potential 4Fe−4S centers, which are present in the glutamate synthase holoenzyme, but not in the isolated subunits. Furthermore, the data demonstrate a specific role of 2-oxoglutarate in promoting electron transfer from FAD to the 3Fe−4S cluster of the glutamate synthase holoenzyme. The modulatory role of 2-oxoglutarate is indeed consistent with the recently determined three-dimensional structure of the glutamate synthase α subunit, in which several polypeptide stretches are suitably positioned to mediate communication between substrate binding sites and the enzyme redox centers (FMN and the 3Fe−4S cluster) to tightly control and coordinate the individual reaction steps [Binda, C., et al. (2000) *Structure 8,* 1299−1308].

Glutamate synthase (GltS,[1] EC 1.4.1.13) is a complex iron−sulfur flavoprotein, which catalyzes the reductive transfer of the L-glutamine amide group to C(2) of 2-oxoglutarate (2-OG) yielding L-glutamate (for a recent review, see ref *1*). On the basis of sequence analyses and comparison

† This work was carried out with funds from the Ministero della Ricerca Scientifica e Tecnologica (PRIN1997 and PRIN 1999) and from the Consiglio Nazionale delle Ricerche (Target Program on Biotechnology), Rome, Italy.

* To whom correspondence should be addressed: Dipartimento di Fisiologia e Biochimica Generali, Universitá degli Studi di Milano, Via Celoria 26, 20133 Milano, Italy. E-mail: mav@mailserver.unimi.it. Phone: +390270644508. Fax: +39022362451.

‡ Universitá degli Studi di Milano.

§ Universitá degli Studi dell' Insubria.

[1] Abbreviations: GltS, glutamate synthase(s); 2-OG, 2-oxoglutarate; 2-IG, 2-iminoglutarate; AADP, 3-aminopyridine adenosine dinucleotide phosphate; ADPRP, adenosine diphosphoribose phosphate; Fd, ferredoxin; L-MetS, L-methionine sulfone; ST, safranin T; PS, phenosafranin; BV, benzyl viologen; MV, methyl viologen; 5-deazaflavin, 5-carba-5-deazariboflavin; E_m, midpoint potential; FAD- and FMNox, -sq, and -hq, oxidized, semiquinone, and hydroquinone forms of FAD and FMN, respectively.

10.1021/bi0100889 CCC: $20.00 © 2001 American Chemical Society
Published on Web 04/14/2001

of known biochemical properties of GltS from different sources, three classes of GltS have been identified in bacteria, photosynthetic cells, and other eukaryotes. *Azospirillum brasilense* GltS is the current model of bacterial GltS, which are NADPH-dependent, are formed by two subunits (the 162 kDa α subunit and the 52.3 kDa β subunit for the *A. brasilense* enzyme), and contain one FAD, one FMN, and three iron−sulfur clusters per catalytically active αβ protomer. During catalysis, NADPH binds at site 1 of GltS (on the β subunit) where it is oxidized with parallel reduction of the enzyme FAD cofactor on this subunit. The electrons flow from FAD to FMN (on the α subunit) through at least two of the three Fe−S centers of GltS [one 3Fe−4S cluster, on the α subunit, and at least one of the two 4Fe−4S centers of the enzyme at an unknown location (*2*)]. At site 2, FMN reduces the postulated 2-imino acid intermediate formed upon addition of ammonia (from L-Gln hydrolysis at the amidotransferase site of the α subunit) and 2-OG (bound at site 2). The eukaryotic pyridine nucleotide-dependent form of GltS is proposed to be structurally and mechanistically similar to the bacterial enzyme in light of the fact that it seems to derive from the fusion of a polypeptide similar to the bacterial β subunit at the C-terminus of a polypeptide similar to the bacterial α subunit. Furthermore, the bacterial GltS α subunit is structurally similar to the ferredoxin-dependent form of GltS of photosynthetic cells. Indeed, in the bacterial enzyme, L-glutamine-dependent glutamate synthesis takes place within the enzyme α subunit (*3*) and the β subunit functions as an FAD-containing NADPH-dependent oxidoreductase (*4*), which has been recruited to make the reducing equivalents available to the α subunit for glutamate synthesis (*1*). In addition, the β subunit appears to be essential for the formation of the 4Fe−4S clusters of the GltS holoenzyme, of which at least one is required for electron transfer between the flavin sites of the enzyme (*2*, *5*). Furthermore, association of the α and β subunits in the αβ holoenzyme has an effect in modulating the properties of the α subunit (*3*). In particular, hydrolysis of glutamine at the amidotransferase site of the α subunit in the absence of 2-oxoglutarate and reductant is abolished in the holoenzyme (*1*, *3*). Finally, the β subunit is the first identified member of a novel class of FAD-dependent NAD(P)H oxidoreductases that form subunits or domains of other complex enzymes, in which the β subunit-like polypeptide also determines the presence of Fe−S clusters with low to very low redox potentials (*1*, *6*, *7*).

To contribute to the understanding of the electron-transfer pathway during the GltS catalytic cycle, we have measured the midpoint potential values of its flavin cofactors and of its 3Fe−4S cluster in the isolated β and α subunits and in the recombinant αβ holoenzyme. To determine if, and to what extent, the state of occupancy of the enzyme catalytic subsites may influence the redox properties of the enzyme cofactors, as also suggested by the recently determined three-dimensional structure of the GltS α subunit (*8*), the experiments were extended to the study of the effect of the presence of enzyme substrates (or substrate analogues) on the oxidoreduction properties of the enzyme cofactors.

MATERIALS AND METHODS

Enzyme Preparation, Protein, and Activity Assays. Preparations of the GltS α and β subunits and of the recombinant GltS holoenzyme were obtained as described in refs *3*−*5*. Prior to each experiment, the enzyme was gel filtered through a Sephadex G-25 (medium) column equilibrated with 25 mM Hepes/KOH buffer (pH 7.5), 10% glycerol, and 1 mM EDTA. Protein concentrations were determined using the Amresco protein assay reagent based on the method of Bradford (*9*) and bovine serum albumin as the reference protein or the known extinction coefficients of the enzyme species [$\epsilon_{454} = 11\ 300\ M^{-1}\ cm^{-1}$ for the β subunit (*4*), $\epsilon_{446} = 21\ 200\ M^{-1}\ cm^{-1}$ for the α subunit (*3*), and $\epsilon_{444} = 62\ 660\ M^{-1}\ cm^{-1}$ for the GltS holoenzyme (*5*, *10*)]. Activity assays were carried out as described previously (*3*, *4*, *11*).

Absorbance Spectroscopy. Absorbance spectra were recorded at 20 °C using a Cary 219 or a Hewlett-Packard HP8453 diode-array spectrophotometer model. Anaerobiosis was achieved using the apparatus and glassware described by Williams et al. (*12*).

Redox Potential Measurements. Redox potential measurements were carried out spectrophotometrically by performing anaerobic reductive titrations of each enzyme species (5−10 μM) in 25 mM Hepes/KOH buffer (pH 7.5), 10% glycerol, and 1 mM EDTA at 20 °C in the presence of a redox indicator dye and a mediator dye (*13*). Different reduction methods were used. Photoreduction was effected by illuminating with a standard projector light the solution, which contained 6−7 mM EDTA and 1 μM 5-carba-5-deazariboflavin [5-deazaflavin (*14*)]. Alternatively, dithionite was added anaerobically from approximately 1 mM anaerobic solutions in the Hepes buffer described above. In some experiments, the xanthine/xanthine oxidase system described by Massey (*15*) was used. The indicator dyes that were found to be suitable for redox potential measurements of GltS cofactors because of their midpoint potential and spectral properties were safranin T [ST, $E_m = -302$ mV, pH 7.5, $n = 2$ (*16*)] and phenosafranin [PS, $E_m = -266$ mV, pH 7.5, $n = 2$ (*16*)]. They were included at concentrations of 5−15 μM. Benzyl viologen [BV, $E_m = -359$ mV, $n = 1$ (*17*)] and methyl viologen [MV, $E_m = -440$ mV, $n = 1$ (*17*)] were used as mediators at concentrations between 0.5 and 10 μM. Control reductive titrations were carried out in the absence of the indicator or of both indicator and mediator dyes.

Data Analysis. For the determination of the midpoint potential of the FAD cofactor bound to the GltS β subunit, absorbance values at 408 nm (where the ST_{ox}/ST_{red} couple has an isosbestic point) were used to monitor the extent of reduction of β subunit-bound FAD. Absorbance values at 521 nm, where the β subunit does not contribute to absorbance, were used to monitor the redox state of the indicator dye. From the rearrangement of the Nernst equations describing the redox behavior of the enzyme-bound FAD (eq 1) and of the indicator dye (eq 2), when the two systems are at equilibrium, n_β was determined from the slope of the log−log plot (eq 3) and the difference between the E_m values of the β subunit cofactor and of the indicator dye was calculated from the vertical intercept of the line (*13*, *15*).

$$E_h = E_{m,\beta} + (59/n_\beta)\log(\beta_{ox}/\beta_{red}) \quad (1)$$

$$E_h = E_{m,dye} + (59/n_{dye})\log(dye_{ox}/dye_{red}) \quad (2)$$

$$\log(\beta_{ox}/\beta_{red}) = (E_{m,dye} - E_{m,\beta})(n_\beta/59) + (n_\beta/n_{dye})\log(dye_{ox}/dye_{red}) \quad (3)$$

$$\epsilon_{obs} = [\epsilon_{ox} \times 10^{(E_h - E_m)(n/59)} + \epsilon_{red}]/[1 + 10^{(E_h - E_m)(n/59)}] \quad (4)$$

$$\epsilon_{obs} = [\epsilon_{FMNox} \times 10^{(E_h - E_{m,FMN})/29.5} + \epsilon_{FMNhq}]/[1 + 10^{(E_h - E_{m,FMN})/29.5}] + [\epsilon_{FeSox} \times 10^{(E_h - E_{m,FeS})/59} + \epsilon_{FeSred}]/[1 + 10^{(E_h - E_{m,FeS})/59}] \quad (5)$$

$$\epsilon_{obs} = [\epsilon_{FMNox} \times 10^{(E_h - E_{m,FMN})/29.5} + \epsilon_{FMNhq}]/[1 + 10^{(E_h - E_{m,FMN})/29.5}] + [\epsilon_{FeSox} \times 10^{(E_h - E_{m,FeS})/59} + \epsilon_{FeSred}]/[1 + 10^{(E_h - E_{m,FeS})/59}] + [\epsilon_{FADox} \times 10^{(E_h - E_{m,FAD})/29.5} + \epsilon_{FADhq}]/[1 + 10^{(E_h - E_{m,FAD})/29.5}] \quad (6)$$

In the equations, the nomenclature is according to Clark (*17*). All values were calculated for 20 °C and pH 7.5. Subscripts indicate the species involved; ϵ_{obs} is the apparent extinction coefficient at 408 nm obtained by dividing A_{408} values during the titration by the enzyme concentration after subtraction of the constant contribution of the indicator dye.

With benzyl viologen as the indicator, the absorbance changes at 454 nm were used to monitor enzyme reduction after correction for the contribution of reduced benzyl viologen. Data were fitted to both eqs 3 and 4. The latter equation correlates the extinction coefficient of the enzyme at a given wavelength (454 nm in this case) to the E_h, calculated with eq 2 from absorbance changes observed at 600 nm during BV reduction, and allows the calculation of the midpoint potential of the cofactor under analysis and the corresponding *n*. The extinction coefficients at 454 nm used for FAD bound to the β subunit were as follows: ϵ_{ox} = 11 300 M^{-1} cm^{-1} and ϵ_{red} = 1470 M^{-1} cm^{-1}.

For the α subunit, where two cofactors (the FMN flavin and the 3Fe−4S cluster) contribute to the absorbance changes observed throughout the reductive titration of the enzyme, absorbance changes at 408 and 521 nm were again used to monitor the redox state of the enzyme and of the indicator dye, respectively. The contribution of each cofactor to absorbance changes observed at 408 nm depends on the relative concentrations of oxidized and reduced species as a function of the redox potential (E_h) and the E_m value of the cofactor (eq 4). Therefore, the absorbance values at 408 nm measured throughout the titration were converted to apparent extinction coefficients (ϵ_{obs}), and the data were fitted to eq 5, which takes into account the contribution of both enzyme chromophores to the absorbance at 408 nm. The extinction coefficients of the various species at 408 nm were calculated from separate experiments (Table 1). ϵ_{FMNox} and ϵ_{FMNhq} were calculated from reductive titrations of free FMN, which were found to yield extinction coefficients similar to those observed during L-glutamate reduction of the FMN cofactor of the GltS α subunit and during flavin bleaching on formation of the FMN−sulfite adduct in the GltS α subunit (*3*). ϵ_{FeSox} and ϵ_{FeSred} were calculated from dithionite titrations of the GltS α subunit after subtraction of the contribution of the oxidized and reduced FMN cofactor (ref *3* and this work). n_{FMN} was assumed to be 2, since no absorbance changes that indicated formation of flavin semiquinone species could be detected during control experiments. n_{FeS} was assumed to be 1. Absorbance values at 521 nm were used directly to determine the E_h value of the system (eq 2) since the α subunit contributes very little to the absorbance of the solution at this wavelength.

Table 1: Summary of Extinction Coefficients Calculated for the GltS Cofactors at 408 nm[a]

	ϵ_{408} (M^{-1} cm^{-1})	
cofactor	oxidized	reduced[b]
FAD	6300 ± 400 (14)	3070 ± 230 (3)
FAD[c]	8120	3280
FMN	7330 ± 240 (17)	3090 ± 200 (3)
3Fe−4S	11800 ± 460 (8)	9390 ± 940 (5)

[a] The values were calculated from several separate experiments (whose number is indicated in parentheses) as described in the text. [b] For FAD and FMN, the extinction coefficients quoted are those of the hydroquinone form. [c] Extinction coefficient of FAD bound to the β subunit−AADP complex from a photoreduction experiment with the enzyme.

For the GltS holoenzyme experiments, eq 5 needed to be expanded to include the contribution of the oxidized and reduced FAD cofactor (eq 6). The extinction coefficients of oxidized and reduced FAD at 408 nm (ϵ_{FADox} and ϵ_{FADhq}, respectively) were determined from reductive titrations of the isolated β subunit (refs *4* and *18* and this work; Table 1). Those of the cofactor in the β subunit−AADP complex were calculated from a photoreduction of the β subunit (approximately 10 μM) in the presence of a 10-fold molar excess AADP. Since no flavin semiquinone radicals were detected during reduction of the β subunit or of the GltS holoenzyme, n_{FAD} was set to 2.

For the measurement of the midpoint potential values of GltS and of its complexes with substrates or their analogues, prior to calculation of E_h values, absorbance changes at 521 nm were corrected to take into account absorbance changes due to reduction of the enzyme or the enzyme−ligand complex, as determined during control reduction experiments in the absence of dyes. Control experiments also determined that no absorbance changes were induced by binding of L-MetS or 2-OG to the enzyme species used (namely, GltS and its isolated α subunit), and that these ligands did not lead to stabilization of flavin semiquinone species or charge-transfer complexes during reduction.

Excel (Microsoft) or Grafit (Erythacus Software) were used for data analysis.

RESULTS AND DISCUSSION

Midpoint Potential of the FAD Cofactor Bound to the GltS β Subunit. The GltS β subunit could be efficiently reduced photochemically, with dithionite or with the xanthine/xanthine oxidase system. No significant absorbance changes attributable to formation of flavin semiquinone species were observed during reductive titrations of the enzyme in the absence or presence of benzyl or methyl viologen. The enzyme was photoreduced in the presence of phenosafranine, safranine T, or benzyl viologen as the indicator dye and methyl viologen as the mediator. Reduction of phenosa-

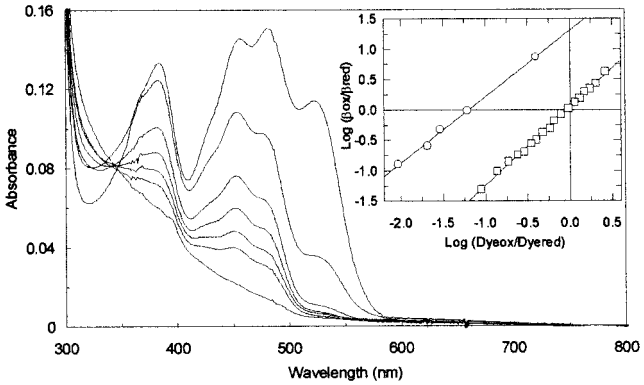

FIGURE 1: Measurement of the midpoint potential value of FAD bound to the isolated β subunit of GltS. The GltS β subunit (10 μM) was photoreduced anaerobically in the presence of 3.3 μM safranin T in 25 mM Hepes/KOH buffer (pH 7.5), 6 mM EDTA, 0.4 μM 5-deazaflavin, 1 μM methyl viologen, and 10% glycerol. The spectra obtained at different times (up to 195 s) of irradiation are shown. The inset shows (○) a log−log plot constructed with the data obtained during the reductive titration shown in the main panel. The data were fitted to eq 3, yielding a line with a slope of 1.1 ± 0.03 and an intercept of 1.3 ± 0.05. The inset also shows (□) data obtained during a reductive titration of 11 μM β subunit in the presence of 10 μM benzyl viologen, 1.8 μM methyl viologen in 25 mM Hepes/KOH buffer (pH 7.5), 1 mM EDTA, and 10% glycerol. Reduction was achieved by the inclusion of xanthine (287 μM) and xanthine oxidase (5 milliunits). The fit of the data to eq 3 yielded a line with a slope of 1.3 ± 0.02 and an intercept of 0.04 ± 0.01.

franine preceded that of the β subunit-bound flavin cofactor, indicating that the midpoint potential value of the enzyme FAD was significantly more negative than that of phenosafranine (not shown). Although safranin T also appeared to have a midpoint potential less negative than that of the FAD bound to the β subunit, it was possible to obtain enough data to correlate the extents of enzyme and dye reduction (Figure 1) and construct a log−log plot (eq 3, Figure 1 inset), which yielded a straight line with a slope of 1 and a calculated midpoint potential for bound FAD of approximately −340 mV (Table 2). A similar midpoint potential value was obtained by using benzyl viologen as the indicator dye and the xanthine/xanthine oxidase system as the reducing system. However, the log−log plot was linear but with a slope of approximately 1.3 (Figure 1 inset). A direct fit of the data to eq 4 yielded a midpoint potential for the enzyme of approximately −347 mV with a noninteger number of transferred electrons ($n = 1.4$, Table 2). Because of the observed non-Nernstian behavior of the enzyme in the presence of benzyl viologen, in the absence of indication of the formation of flavin semiquinone species, we decided to abandon the use of this dye as the indicator.

To test the effect of the presence of the pyridine nucleotide substrate and/or product on the redox behavior of the GltS β subunit, redox titrations were repeated in the presence of excess AADP, a nonreducible analogue of $NADP^+$, which binds tightly to the GltS β subunit ($K_d = 1.1$ μM) and perturbs the flavin absorbance spectrum (*18*). In a control experiment, the β subunit−AADP complex was photochemically reduced in the absence of the indicator dye. A small absorbance increase at wavelengths of >515 nm was observed. This absorption band was attributed to formation of a charge-transfer complex between FAD_{hq} and AADP rather than to accumulation of flavin semiquinone because

Table 2: Summary of the Midpoint Potential Values Calculated for the Flavin Cofactors and the 3Fe−4S Cluster of GltS[a]

			E_m (mV)		
enzyme	ligand	dye	FAD ($n = 2$)	FMN ($n = 2$)	3Fe−4S ($n = 1$)
β subunit	none	ST	-340 ± 1.5		
β subunit[b]	none	BV[b]	-347 ± 0.5[b]		
β subunit	AADP	ST	-307 ± 0.4		
β subunit	AADP	ST	-313 ± 0.2		
β subunit	ADPRP	ST	-351 ± 2.4		
α subunit	none	PS		-236 ± 1.4	-264 ± 3.0
α subunit	L-MetS	PS		-249 ± 1.9	-251 ± 4.3
α subunit	2-OG	PS		-237 ± 1.4	-285 ± 3.0
GltS	none	PS/ST	-299 ± 4.7	-237 ± 3.6	-280 ± 11.2
GltS	AADP	PS/ST	-308 ± 1.6	-229 ± 2.7	-259 ± 5.3
GltS	L-MetS	PS/ST	-305 ± 2.8	-230 ± 2.8	-261 ± 6.6
GltS	2-OG	PS/ST	-299 ± 1.0	-267 ± 1.4	-188 ± 9.2

[a] All measurements were carried out at pH 7.5 and 20 °C under conditions described in detail in the text. n is the number of transferred electrons during reduction of the cofactor. [b] The GltS β subunit was reduced with the xanthine/xanthine oxidase system in the presence of benzyl viologen as the indicator dye and methyl viologen as the mediator (*15*). Data from two separate experiments were fitted directly to eq 4 using absorbance changes at 600 nm to determine E_h according to eq 2. A value for n_{FAD} of 1.4 was obtained.

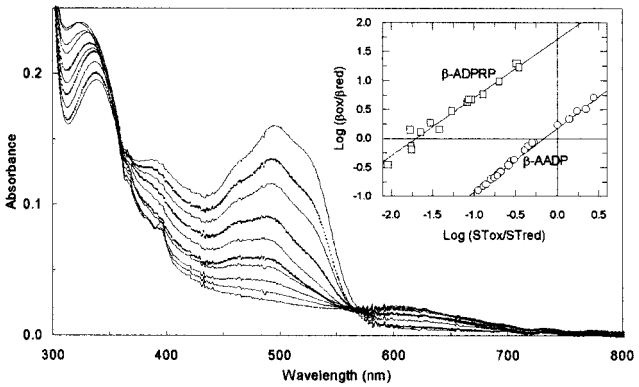

FIGURE 2: Effect of AADP and of ADPRP on the redox properties of the GltS β subunit. In the main panel, 11.7 μM β subunit was photoreduced in the presence of 68 μM AADP, 3.1 μM safranin T, 6 mM EDTA, 0.9 μM deazaflavin, 1.3 μM methyl viologen in 25 mM Hepes/KOH buffer (pH 7.5), and 10% glycerol at 20 °C. For the sake of clarity, only some of the spectra obtained during the photoreduction experiment (up to a total of 200 s of irradiation) are shown in the figure. The inset shows (○) a log−log plot of the data obtained during the experiment shown in the main panel. The line is the best fit of the data to eq 3 that yielded a slope of 1.1 ± 0.02 and an intercept of 0.2 ± 0.01. The inset also shows (□) a log−log plot of the data obtained during a reductive titration of the GltS β subunit (8.3 μM) in the presence of ADPRP (140 μM). All other conditions were similar to those of the experiment shown in the main panel. The line is the best fit of the data to eq 3 and has a slope of 1.0 ± 0.05 and an intercept of 1.7 ± 0.1.

of the shape of the band and because of the fact that it did not disappear at long irradiation times, which would have led to full reduction of a flavin semiquinone to the hydroquinone species. The data obtained during redox titrations of the β subunit−AADP complex in the presence of safranin T as the indicator dye (Figure 2) were analyzed with particular care to determine the effect of the absorbance changes at wavelengths above 515 nm on the calculation of the extent of dye reduction. Log−log plots constructed using absorbance changes at several wavelengths between 512 and 540 nm to monitor dye reduction gave essentially the same results. The calculated midpoint potential value was ap-

proximately −310 mV (Table 2), thus 30 mV less negative than that measured with the free enzyme.

In contrast with the effect of binding of AADP to the enzyme on both the absorbance spectrum and the redox properties of the GltS β subunit, ADPRP, the NADP(H) analogue lacking the nicotinamide ring, did not induce any absorbance changes when it was added to the enzyme solution at a concentration of up to 140 μM (not shown), although it is known to inhibit the GltS β subunit [$K_i \approx 20$ μM (*4*, *18*)]. The redox behavior of the enzyme-bound flavin also appeared to be unaffected by ADPRP, and the calculated midpoint potential of the bound flavin was −351 ± 2.4 mV (inset of Figure 2 and Table 2).

Overall, in the β subunit, there appears to be a specific effect of the charge-transfer interaction between the reduced flavin isoalloxazine ring and the NADP(H) nicotinamide ring, which stabilizes the hydroquinone form of the flavin. This effect suggests that it is through formation of a charge-transfer complex between the reduced flavin and the pyridine nucleotide that electron transfer from the pyridine nucleotide to the enzyme FAD cofactor is favored during catalysis.

Midpoint Potential of the FMN Cofactor and of the 3Fe−4S Cluster Bound to the GltS α *Subunit.* During reductive titrations of the GltS α subunit, we found that photoreduction led to enzyme inactivation (*3*), which is most likely due to destruction of the enzyme 3Fe−4S cluster as judged by comparison of absorbance spectra of the native enzyme and of that recovered after photoreduction and air reoxidation. Dithionite was instead found to reduce the enzyme redox centers efficiently with essentially complete recovery of both the initial absorbance spectrum of the enzyme and enzyme activity at the end of the experiments. Therefore, the enzyme was titrated with dithionite in the presence of safranin T or phenosafranine, the latter being the dye that allowed us to determine the midpoint potential values of GltS α subunit cofactors in the free enzyme and in the GltS−L-MetS or GltS−2-OG complexes (Figure 3). Absorbance changes at 408 nm could be fitted to eq 5, which yielded estimates of the midpoint potential values of the bound FMN cofactor and the 3Fe−4S cluster (Table 2). In this equation, the following assumptions were made: (a) No FMN semiquinone species is formed throughout the titration, as shown by control redox titrations under a variety of conditions and in the absence of the indicator dye, so that *n* for the flavin was set to 2, and (b) the flavin and the Fe−S cluster were reduced independently from each other. The latter assumption was supported by the observation that the two redox centers of the α subunit of GltS do not seem to be able to equilibrate with each other (*3*) and by the fact that eq 5 fitted the data well. The calculated midpoint potential values for the free α subunit were approximately −240 mV for FMN and −260 mV for the 3Fe−4S cluster (Table 2). L-MetS, a glutamine analogue, and 2-OG had no significant effect on the calculated midpoint potential of the FMN cofactor (Table 2 and Figure 3). L-MetS also had little effect on the midpoint potential of the 3Fe−4S cluster (Table 2 and Figure 3). On the contrary, the midpoint potential of the 3Fe−4S center was sensitive to the presence of 2-OG, which caused an approximately 20 mV decrease in the measured value (Table 2 and Figure 3).

As a whole, these experiments confirm that in the free α subunit the midpoint potential values of FMN and of the

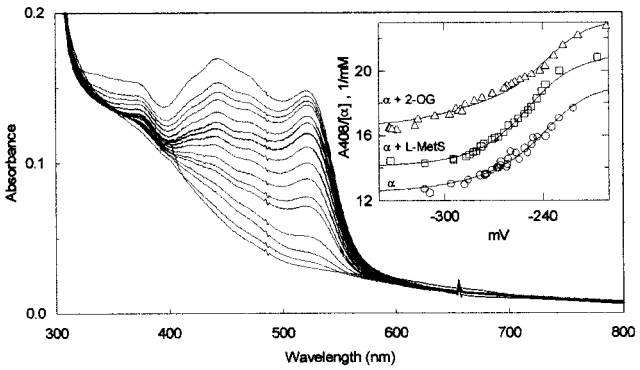

FIGURE 3: Measurement of the midpoint potential value of the FMN cofactor and of the 3Fe−4S center bound to the isolated α subunit of GltS. In the main panel, the GltS α subunit (7.3 μM) was anaerobically titrated with a dithionite solution (0.74 mM) in the presence of 3.9 μM phenosafranin and 1 μM benzyl viologen. The inset shows the absorbance changes at 408 nm, after correction for the dye contribution and normalization, plotted as a function of solution potential (in millivolts), as determined from absorbance changes at 521 nm. The curves are the best fit of the data to eq 5 using the extinction coefficients summarized in Table 1. The E_m values shown in Table 2 were obtained. (○) Data from three separate titrations of the α subunit similar to the one shown in the main panel. (□) Data from the titration of the α subunit in the presence of 1 mM L-MetS (the apparent extinction coefficients and the fitted curve have been offset by 2 units). (△) Data from a titration of the GltS α subunit in the presence of 1 mM 2-OG (the apparent extinction coefficients and the fitted curve have been offset by 4 units for clarity).

3Fe−4S cluster do not differ from each other sufficiently to be reduced in well-separated phases (*3*). It is also confirmed that the two centers appear to be reduced independently from each other and that no detectable amounts of flavin semiquinones accumulate during reduction. The latter observation indicates that the midpoint potential of the FMN_{ox}/FMN_{sq} couple must be at least 100−120 mV more negative than that of the FMN_{sq}/FMN_{hq} couple; with a 120 mV separation in potential, up to approximately 5% of a flavin semiquinone species would have accumulated during the titration (*17*) and could have been detected during our experiments. Thus, assuming that the two redox couples are separated by 120 mV, we can estimate from the midpoint potential of the FMN_{ox}/FMN_{hq} couple of the free enzyme (approximately −240 mV) that the E_m values of the FMN_{ox}/FMN_{sq} and FMN_{sq}/FMN_{hq} couples are approximately −300 and −180 mV, respectively. These values, together with that of the 3Fe−4S cluster, which ranges from −250 to −285 mV, depending on the state of ligation of the α subunit (Table 2), provide a thermodynamic explanation for the fact that when the GltS α subunit was reduced with excess L-glutamate we could observe reduction of FMN but not of the 3Fe−4S cluster (*3*). Indeed, one-electron transfer from reduced FMN to the oxidized 3Fe−4S cluster is most likely prevented by the at least 70 mV unfavorable potential difference of the species involved (FMN_{sq}/FMN_{hq} and $3Fe-4S_{ox}/3Fe-4S_{red}$ couples). The data presented here may also explain, at least in part, the observation that when the dithionite-reduced α subunit was reacted with a molar excess of 2-OG and L-glutamine only FMN oxidation was observed (*3*). The one-electron-transfer process between the reduced 3Fe−4S cluster and oxidized FMN (to yield FMN_{sq}) would be unfavored due to the 15−50 mV difference existing between the redox couples that are involved. However,

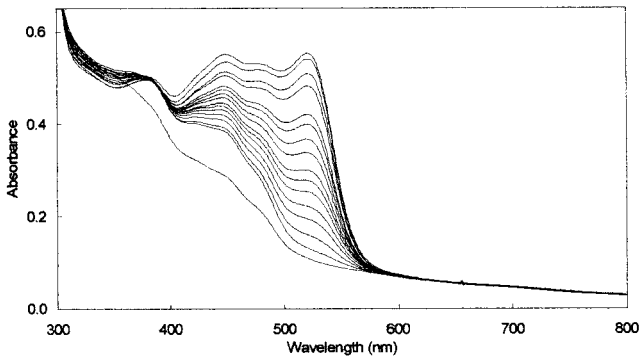

FIGURE 4: Determination of the midpoint potential of the GltS−2-oxoglutarate complex in the presence of phenosafranin. GltS (7.6 μM) was photoreduced anaerobically in 25 mM Hepes/KOH buffer (pH 7.5) and 10% glycerol in the presence of 1 mM 2-OG, 8.9 mM EDTA, 1 μM 5-deazaflavin, 16 μM phenosafranin, and 0.5 μM methyl viologen. Spectra obtained at equilibrium after up to 720 s of irradiation are shown.

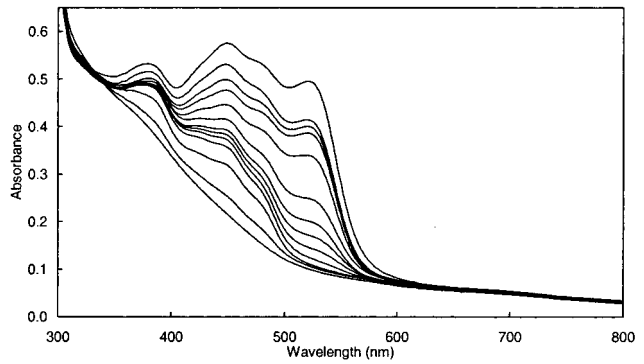

FIGURE 5: Determination of the midpoint potential of the GltS−L-methionine sulfone complex in the presence of safranin T. GltS (8. 2 μM) in 25 mM Hepes/KOH buffer (pH 7.5), 1 mM EDTA, 10% glycerol, 1 mM L-MetS, 13 μM safranin T, and 0.4 μM methyl viologen was made anaerobic and reduced by adding aliquots of an anaerobic dithionite solution (3.2 mM). Shown are the dilution-corrected spectra obtained at equilibrium after addition of up to 26 μL of dithionite solution.

electron transfer may indeed take place from the reduced 3Fe−4S cluster and the oxidized FMN cofactor generating FMN_{sq} against a potential difference provided the (unstable) FMN_{sq} could be converted to the (stable) FMN_{hq} species by acquiring a second electron directly or indirectly (e.g., through the Fe−S cluster) from another α subunit molecule. The fact that this does not happen in our experiment implies that intermolecular electron transfer is not possible in a GltS α subunit solution.

Midpoint Potential of the FAD and FMN Cofactors and of the 3Fe−4S Cluster of the GltS Holoenzyme. The midpoint potential values calculated for FAD bound to the isolated β subunit and for FMN and the 3Fe−4S cluster of the α subunit were sufficiently separated from each other so that two different indicator dyes had to be used: safranin T for FAD and phenosafranine for FMN and the 3Fe−4S cluster. We reasoned that if the association of the two subunits in the GltS αβ protomer did not lead to major changes in the redox behavior of the cofactors, it could be possible to determine the midpoint potential values of FMN and of the 3Fe−4S cluster of the GltS αβ holoenzyme by using phenosafranine as the indicator dye, and of FAD by performing reductive titrations in the presence of safranine T. Photoreduction (*5*) of the GltS αβ holoenzyme suggested that this was the case.

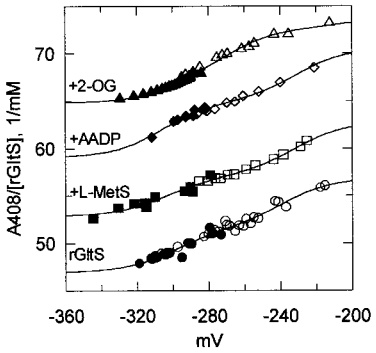

FIGURE 6: Determination of the midpoint potential values of the flavin cofactors and the 3Fe−4S cluster of the GltS holoenzyme free or in complex with substrates or substrates analogues. The GltS holoenzyme (4−8 μM) was photoreduced (in the presence of 7−8 mM EDTA and 1 μM deazaflavin) or chemically reduced with dithionite (from 1 to 3 mM solutions) in the presence of methyl viologen (0.5−1 μM) as the mediator dye and either phenosafranin (4−16 μM, white symbols) or safranin T (5−15 μM, black symbols) as the indicator dye. The curves are the best fit of the data to eq 6 using the extinction coefficients shown in Table 1 and yielding the values summarized in Table 2. For the GltS holoenzyme, data from three separate experiments with each dye were fitted together to eq 6 (circles). GltS in the presence of 1 mM L-MetS (squares). The data and the fitted curve have been offset by 6 units for clarity. GltS in the presence of 90 μM AADP (diamonds). The data and the curve have been offset by 12 units. GltS in the presence of 1 mM 2-OG (triangles). The data and the curve have been offset by 18 units for clarity.

Indeed, it took place in three phases. First, absorbance changes similar to those observed during reduction of the isolated α subunit were obtained. These changes were followed by absorbance changes similar to those observed during reduction of the GltS β subunit. Finally, reduction of the enzyme 4Fe−4S clusters seemed to take place. The results are in agreement with previous low-temperature EPR spectroscopy experiments on GltS prepared from *Azospirillum* cells (*2*). Both 4Fe−4S clusters of GltS exhibited low to very low midpoint potentials; center II was only partially reduced by anaerobic addition of a molar excess NADPH and quantitatively reduced in the presence of a NADPH-regenerating system and by the light/deazaflavin system. The second 4Fe−4S cluster of GltS (center III) could only be reduced photochemically so that its role in the enzyme-catalyzed reaction is still unclear. Dithionite reduction of the recombinant GltS αβ holoenzyme yielded results similar to those observed during photochemical reduction with respect to the first two parts of the reduction, but it did not seem to reduce the 4Fe−4S clusters of the enzyme, in agreement with previous results (*2*).

As expected, the redox potential range explored by using phenosafranin as the indicator dye, and dithionite or the light/deazaflavin system as the reductant, allowed us to monitor reduction of the FMN and 3Fe−4S cluster bound to the α subunit, while changes observed during redox titrations in the presence of safranin T monitored mainly FAD reduction (Figures 4−6). The redox behavior of the enzyme was found to be independent of the reduction method used (dithionite reduction or photoreduction) as well as of the concentrations of the indicator dyes, of varying concentrations of methyl viologen, and of the additional presence of benzyl viologen at a low concentration. Finally, the enzyme reductive titration appeared to be reversible; in some cases, the fully reduced solution was allowed to slowly reoxidize over a period of

24 or even 48 h due to reaction with oxygen that leaked into the cuvette over long periods of time. The data obtained during such reoxidations were essentially superposable with those gathered during reduction. However, only data obtained during reductive titrations were used for E_m value calculations to avoid artifacts due to minor protein inactivation and/or denaturation or dye degradation during incubation for 1−2 days at 20 °C. The data from several experiments were analyzed using eq 6, which includes the contribution of the three redox centers to the observed absorbance changes at 408 nm. The estimated values of the midpoint potentials of FAD, FMN, and the 3Fe−4S cluster are approximately −300, −240, and −280 mV, respectively (Table 2). These values are similar to those calculated for the same cofactors in the isolated subunits (Table 2) with the exception of the calculated midpoint potential value of FAD, which was approximately 40 mV less negative in the holoenzyme with respect to the isolated β subunit. At variance with the isolated β subunit, the effect of the presence of AADP was negligible (Table 2). AADP binding to the GltS holoenzyme is indeed tight ($K_d \approx 2$ μM, not shown) and induces absorbance changes that are qualitatively and quantitatively similar to those observed with the β subunit (*18*), indicating that the mode of binding of AADP to the pyridine nucleotide site of GltS is similar to that of the β subunit. The lack of an effect of AADP on the measured E_m of the holoenzyme as opposed to the isolated β subunit may rather correlate with the different tendency of the two enzymes to form a stable charge-transfer complex between FAD_{hq} and $NADP^+$ or its analogue, AADP. The reduced isolated β subunit forms a stable charge-transfer complex with $NADP^+$ (*4*) and, as reported above, with AADP. Reduction of the GltS holoenzyme with NADPH led to essentially no formation of a similar charge-transfer complex, and photoreduction of GltS in the presence of AADP brought about absorbance changes at long wavelengths that were hardly detectable, thus much lower than those observed with the β subunit (Figure 2).

As observed for the isolated α subunit, L-MetS had no dramatic effect on the behavior of the enzyme redox centers (Table 2). In contrast with what was observed with the isolated α subunit, 2-OG induced marked changes in the calculated E_m values of the 3Fe−4S cluster and of the FMN cofactor. In the presence of 2-OG, the 3Fe−4S center of GltS exhibited a midpoint potential significantly less negative ($E_m \approx -190$ mV) than in the absence of the substrate ($E_m \approx -280$ mV), while that of FMN was lowered by approximately 30 mV. This observation was confirmed by a dithionite titration of the GltS−2-OG complex in the absence of the indicator dyes; during the early stages of reduction, absorbance changes were consistent with reduction of the cluster only (not shown) as opposed to concomitant reduction of one enzyme flavin and the 3Fe−4S center observed with the free enzyme (ref *5* and this work) or in complex with other substrate analogues (not shown). How the 2-OG effect may favor catalysis during GltS reaction will be discussed below.

CONCLUSIONS

The midpoint potential values of the FAD and FMN flavin cofactors of GltS and of its 3Fe−4S cluster have been determined. Only the value of the midpoint potential of FAD is significantly affected by the association of the α and β subunits of the enzyme in forming the GltS $\alpha\beta$ protomer; such a value becomes less negative, and thus, the change is in a direction that favors GltS reduction by NADPH. This finding is consistent with the proposal that limited but significant conformational changes do take place on association of the two subunits to form the catalytically active $\alpha\beta$ holoenzyme (*1*, *3*).

The calculated midpoint potential values of GltS flavins and the 3Fe−4S cluster are consistent with overall electron transfer from NADPH to FAD (at site 1 of GltS on its β subunit) to the 2-iminoglutarate intermediate (at site 2 on the α subunit) through FMN, and with the participation of the 3Fe−4S cluster of the enzyme in the intramolecular electron-transfer process between the flavin sites. The midpoint potential values calculated for FMN and the 3Fe−4S cluster of GltS are also in the range of values reported for the spinach ferredoxin (Fd)-dependent enzyme, supporting the overall functional and structural similarity between the GltS α subunit and the single-subunit Fd-dependent enzyme. However, for spinach Fd-dependent GltS, the two centers were reported to be equipotential (−225 mV; *19*), while with the GltS holoenzyme and its α subunit, we could distinguish between FMN and 3Fe−4S cluster reduction and detect differences in their midpoint potential values (Table 2).

AADP appears to form a stable charge-transfer complex with reduced FAD bound to the β subunit, which, in the isolated subunit, favors flavin reduction. This complex, as well as the charge-transfer complex between reduced FAD and $NADP^+$, is formed to a very low extent in the GltS holoenzyme, and may explain why the presence of AADP has no detectable effect on the E_m value of FAD bound to the holoenzyme.

L-MetS causes no significant changes in the midpoint potential of the redox centers of the α subunit in both the isolated subunit and the holoenzyme. On the contrary, 2-oxoglutarate, which binds at site 2 of GltS next to FMN and the 3Fe−4S center (*8*), has a different effect on the redox behavior of FMN and of the 3Fe−4S cluster depending on the protein species under analysis. In the isolated α subunit, the presence of 2-OG has no effect on FMN but lowers the 3Fe−4S cluster E_m value. In the holoenzyme, 2-OG causes a significant (≈100 mV) increase in the E_m value of the 3Fe−4S cluster and a 30 mV decrease in that of the FMN_{ox}/FMN_{hq} couple.

The effect of the ligands of the α subunit on the E_m values of the cofactors of this subunit is particularly interesting in light of the three-dimensional structure of the GltS α subunit, which has been recently obtained by X-ray diffraction analysis of protein crystals (*8*). As described in detail elsewhere (*8*), it appears that several loops of the α subunit may have a role in communicating the correct ligation and redox state between the glutamine amidotransferase site and the site of glutamate synthesis so that only when substrates are bound and reducing equivalents are available, glutamine hydrolysis takes place at the amidotransferase site, ammonia is transferred to the 2-oxoglutarate site through the solvent-shielded intramolecular tunnel, and the 2-iminoglutarate intermediate is reduced to yield the L-glutamate product. The experiments presented here clearly demonstrate that in the holoenzyme the redox behavior of the enzyme flavins and of the 3Fe−4S cluster are essentially insensitive to the state

of occupancy of the amidotransferase domain and of the pyridine nucleotide binding site. No structural information is available yet about the β subunit of GltS or about the GltS $\alpha\beta$ holoenzyme so that no comments can be made at this stage about how the presence of the pyridine nucleotide may be sensed by site 2 and by the glutamine amidotransferase site of GltS. However, with the structure of the α subunit at hand (*8*), the lack of an effect of L-MetS on the redox properties of the α subunit cofactors indicates that despite the presence of a loop (residues 470−520), which makes contacts with residues in the glutamine and 2-OG binding sites and residues interacting with the redox centers (*8*), the state of occupancy of the glutamine site has no marked regulatory effect on the redox properties of the enzyme cofactors. The data presented here, however, clearly indicate that 2-OG may be mainly responsible for regulation of the redox reactivity of the enzyme cofactors within the α subunit at the site of 2-OG binding and L-glutamate synthesis, and that the 2-OG effect plays a relevant role in GltS catalysis.

Again this finding is consistent with structural data (*8*), which show that 2-OG binds in front of the FMN isoalloxazine ring and is held in place by several electrostatic interactions with residues of loops 4 and 6 of the GltS α subunit (*8*), which form (or are in contact with) the FMN cofactor and the 3Fe−4S cluster binding sites.

A scheme describing the electron-transfer process, which takes place during the GltS reaction, can indeed be proposed by taking into account the data gathered during the experiments described here (Figure 7). In this scheme, the E_m values of the $NADP^+$/NADPH and (2-OG + NH_3)/L-Glu couples are set to approximately −340 and −126 mV, respectively (*20*). Second, estimates for the $flavin_{ox}/flavin_{sq}$ and $flavin_{sq}/flavin_{hq}$ couples could be calculated from the E_m values of the corresponding $flavin_{ox}/flavin_{hq}$ couples by taking into account the fact that no flavin semiquinone species could be detected during these experiments. The observation is consistent with the fact that the midpoint potential value of each $flavin_{ox}/flavin_{sq}$ couple is at least 100−120 mV more negative than that of the corresponding $flavin_{sq}/flavin_{hq}$ couple (*17*). Using 120 mV as the E_m difference between the couples, we can calculate approximate midpoint potential values for the FAD_{ox}/FAD_{sq} (−360 mV), FAD_{sq}/FAD_{hq} (−240 mV), FMN_{ox}/FMN_{sq} (−300 mV in the free GltS holoenzyme and −330 mV in the complex with 2-OG), and FMN_{sq}/FMN_{hq} couples (−180 mV for free GltS and −210 mV for the 2-OG complex). Finally, it is assumed that the 3Fe−4S cluster and one of the 4Fe−4S centers of GltS [FeS in Figure 7, corresponding to GltS center II, the 4Fe−4S cluster that is reduced with NADPH (*2*)] are involved in the process. With this information and the values of the midpoint potential of the 3Fe−4S cluster, we can propose the following pathway for electrons during GltS reaction. NADPH bound at site 1 of GltS is oxidized with parallel reduction of FAD to the hydroquinone species (step 1 of Figure 7). One-electron transfer from FAD_{hq} to the 3Fe−4S cluster takes place in step 2, which is unfavored in the absence of bound 2-OG (Figure 7A) but strongly favored in its presence (Figure 7B). This one-electron-transfer process generates FAD_{sq} at a potential low enough to reduce center II of GltS in step 3. At this stage, the potential of center II can be sufficiently negative (perhaps in the range of −360 mV) to allow electron transfer to FMN, generating the

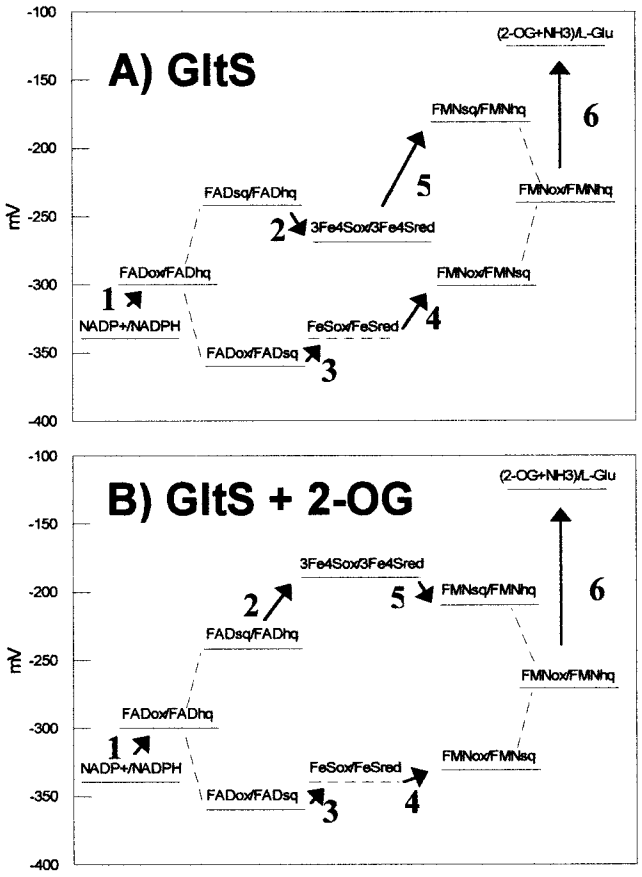

FIGURE 7: Proposed electron-transfer pathway during the GltS-catalyzed reaction. (A) Midpoint potential values determined with free GltS or with GltS in complex with AADP or L-MetS. (B) Midpoint potential values calculated for the GltS−2-OG complex. Numbers indicate reaction steps as described in the text. FeS represents center II of GltS, the 4Fe−4S center that is reduced with NADPH (*2*) whose midpoint potential is low but undetermined as indicated by the horizontal dashed line. Also, the estimates of midpoint potential values of the $flavin_{ox}/flavin_{sq}$ and $flavin_{sq}/flavin_{hq}$ couples are indicated with dashed lines.

(unstable) FMN_{sq} species (step 4). In step 5, FMN_{sq} is converted into FMN_{hq} by receiving one electron from the reduced 3Fe−4S center. This step is thermodynamically uphill if 2-OG is bound, or if the 2-iminoglutarate intermediate (2-IG) formed on addition of ammonia from glutamine hydrolysis to 2-OG has the same effect as 2-OG on the midpoint potential of both the 3Fe−4S center and FMN (Figure 7B), but it may be driven by the subsequent reoxidation of FMN upon two-electron transfer to 2-IG (step 6). In this case, the lowered E_m of the FMN_{ox}/FMN_{hq} couple in the presence of 2-OG may help in driving the reaction. Alternatively, 2-IG may be formed between steps 4 and 5, and it may cause a shift in potential, which brings back the values to those measured in the free enzyme (Figure 7A). In this case, both steps 5 and 6 would be thermodynamically favored.

Indeed, this scheme is consistent with data available so far on the GltS reaction mechanism. In particular, it is consistent with the tight control exerted by the enzyme on release of ammonia from glutamine, its transfer to the 2-OG site, with formation of the imino acid intermediate, which is efficiently converted to L-glutamate. As a result, wasteful consumption of glutamine (or even reducing equivalents) is avoided (*21*).

The recent identification of conditions that allow us to produce significant amounts of recombinant *Azospirillum* GltS should make possible the extension of these studies to the in-depth characterization of the 4Fe−4S clusters of GltS and the application of rapid reaction techniques to the study of this complex iron−sulfur flavoprotein.

REFERENCES

1. Vanoni, M. A., and Curti, B. (1999) *Cell. Mol. Life Sci. 55*, 617−638.
2. Vanoni, M. A., Edmondson, D. E., Zanetti, G., and Curti, B. (1992) *Biochemistry 31*, 4613−4623.
3. Vanoni, M. A., Fischer, F., Ravasio, S., Verzotti, E., Edmondson, D. E., Hagen, W. R., Zanetti, G., and Curti, B. (1998) *Biochemistry 37*, 1828−1838.
4. Vanoni, M. A., Verzotti, E., Zanetti, G., and Curti, B. (1996) *Eur. J. Biochem. 236*, 937−946.
5. Stabile, H., Curti, B., and Vanoni, M. A. (2000) *Eur. J. Biochem. 267*, 2720−2730.
6. Rosenbaum, K., Jahnke, K., Curti, B., Hagen, W. R., Schnackerz, K., and Vanoni, M. A. (1998) *Biochemistry 37*, 17598−17609.
7. Hagen, W. R., Silva, P. J., Amorim, M. A., Hagedoon, P. L., Wassink, H., Haaker, H., and Robb, F. T. (2000) *J. Biol. Inorg. Chem. 5*, 527−534.
8. Binda, C., Bossi, R., Wakatsuki, S., Artz, S., Coda, A., Curti, B., Vanoni, M. A., and Mattevi, A. (2000) *Structure 8*, 1299−1308.
9. Bradford, M. M. (1976) *Anal. Biochem. 72*, 248−254.
10. Vanoni, M. A., Negri, A., Zanetti, G., Ronchi, S., and Curti, B. (1990) *Biochim. Biophys. Acta 1039*, 374−377.
11. Vanoni, M. A., Nuzzi, L., Rescigno, M., Zanetti, G., and Curti, B. (1991) *Eur. J. Biochem. 202*, 181−189.
12. Williams, C. H., Arscott, L. D., Matthews, R. G., Thorpe, C., and Wilkinson, K. D. (1979) *Methods Enzymol. 62*, 185−207.
13. Minneart, K. (1965) *Biochim. Biophys. Acta 110*, 42−56.
14. Massey, V., and Hemmerich, P. (1978) *Biochemistry 17*, 9−17.
15. Massey, V. (1991) in *Flavins and Flavoproteins* (Curti, B., Ronchi, S., and Zanetti, G., Eds.) pp 59−66, de Gruyter, Berlin.
16. Hunt, J., Massey, V., Dunham, W. R., and Sands, R. H. (1993) *J. Biol. Chem. 268*, 18685−18691.
17. Clark, W. M. (1960) in *Oxidation-reduction potentials of organic systems*, Williams and Wilkins Co., Baltimore.
18. Morandi, P., Valzasina, B., Colombo, C., Curti, B., and Vanoni, M. A. (2000) *Biochemistry 39*, 727−735.
19. Hirasawa, M., Hurley, J. K., Salamon, Z., Tollin, G., and Knaff, D. B. (1996) *Arch. Biochim. Biophys. 330*, 209−215.
20. Engel, P. C., and Dalziel, K. (1967) *Biochem. J. 105*, 691−695.
21. Vanoni, M. A., Edmondson, D. E., Rescigno, M., Zanetti, G., and Curti, B. (1991) *Biochemistry 30*, 11478−11484.

BI0100889